# Rigorous diffraction of an electromagnetic beam by wavelength-size slits

J. Sumaya-Martínez
*Facultad de Ciencias. Universidad Autónoma del Estado de México.*
*Av. Instituto Literario No. 100, Toluca. Estado de México, 50000, Mexico.*

O. Mata-Méndez and F. Chavez-Rivas
*Departamento de Física, Escuela Superior de Física y Matemáticas.*
*Instituto Politécnico Nacional, Zacatenco. México, D.F., 07738, Mexico.*

A rigorous modal theory for the diffraction of Gaussian beams from *N* slits in an otherwise perfectly plane conducting screen (line finite-grating) is presented. The case of normal incidence and T.E.-polarization is considered, i.e. the electric field is parallel to the strips. The characteristics of the far-field radiation pattern as a function of the wavelength are analyzed, particularly within the vectorial region where the influence of polarization is more important. Furthermore, the influence of the beam width and beam alignment on the transmission coefficient, on the normally diffracted energy, and on the diffraction is studied.

*Keywords:* Diffraction, scattering; Electromagnetic optics; Gratings; Optics physics

## 1. Introduction

The diffraction of beam waves has attracted a great deal of attention in recent years, particularly in visible and microwave regions because of their applications in optics [1-4] and in solid state physics [5,6]. Particular attention has been devoted to Gaussian beams [7-11] since is the basic emission mode of a laser [12]. Although there have been vast number of investigations of diffraction by a single slit (or strip) and gratings in a plane, the case of several slits (finite line-grating) has not been examined rigorously. As approximate methods, a Kirchhoff-type and the Keller geometrical theory of diffraction [13] are usually used; however, an electromagnetic rigorous theory is necessary in order to obtain accurate results. In this paper generalizing the modal method used in the study of the diffraction by one [6,7] and two slits [4] a rigorous modal theory for the diffraction of an electromagnetic beam by *N* equally spaced slits of width $\ell$ and spacing $D$ ruled in an otherwise perfectly conducting thin plane is presented. This theory works well both in the scalar as in the vectorial region [4], though the latter case will be analyzed with more detail. A diffraction problem such as this is not only an interesting subject in the field of electromagnetic wave theory but also an important one relating to the surface measurement or diagnostics by microwave, millimeter-wave, laser, or ultrasonic beams, and specially to the development of various kinds of optical devices [14].
Finally, it is important to mention that although several rigorous theories can be found in the literature only the case of incident plane waves has been considered [15-19].

The organization of the material is as follows. The theory that leads to the solution of the scattering and diffraction of TE-polarized electromagnetic beams by a finite line-grating is presented in Section 2. In Section 3, the diffraction of normally incident Gaussian beams is numerically analyzed as a function of several optogeometrical parameters. The transmission coefficient and the energy diffracted normally to the screen are also studied. The parameters considered in the analysis are the number of slits, the wavelength, as well as the width and position of the beam waist. Concluding remarks are given in Section 4.

## 2. Theory

### *2.1 The angular spectrum of plane waves*

Consider *N* equally spaced slits of width $\ell$, separation $d$, and spacing $D$ $(=\ell+d)$ ruled on a flat, perfectly conducting thin screen (see Fig. 1) placed in vacuum. The system is illuminated by a TE-polarized Gaussian beam at normal incidence, which is independent of the *z*-coordinate (cylindrical wave). The complex representation of field quantities is used and the complex time term $\exp(-iwt)$ is omitted from now on.

The uniqueness of the solution and the invariance of the field along the *z*-coordinate means that the total field $\mathbf{E}$ depends only on the coordinates *x* and *y*, thus the two-dimensional Helmholtz equation should be satisfied

$$\frac{\partial^2 E}{\partial x^2}+\frac{\partial^2 E}{\partial y^2}+k_0^2 E=0\,. \qquad (1)$$

We assume that the field $E(x,y)$ can be Fourier analyzed as a function of *x*, i.e. we can write,

$$E(x,y)=\frac{1}{\sqrt{2\pi}}\int_{-\infty}^{\infty}\hat{E}(\alpha,y)\exp(i\alpha x)d\alpha\,, \qquad (2)$$

where $\hat{E}(\alpha,y)$ is given by

$$\hat{E}(\alpha,y)=\frac{1}{\sqrt{2\pi}}\int_{-\infty}^{\infty}E(x,y)\exp(-i\alpha x)dx\,. \qquad (3)$$

Substitution of Eq. (2) into the Helmholtz equation (1) yields to a second order differential equation in $\hat{E}(\alpha,y)$, with solution

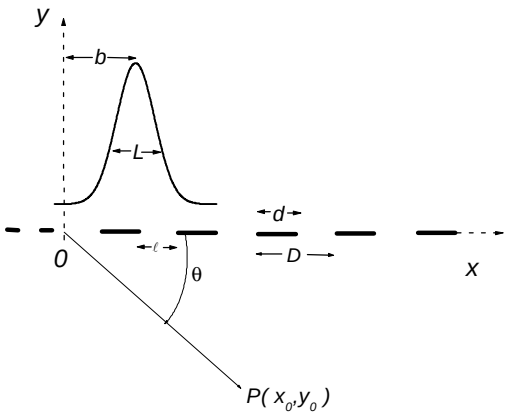


**Figure 1.** Our system composed by *N* slits with uniform width.

$$\hat{E}_1(a,y) = A(a)\exp(-iby) + B(a)\exp(iby) \qquad (4)$$

for $y > 0$, and

$$\hat{E}_2(a,y) = C(a)\exp(-iby) + D(a)\exp(iby) \qquad (5)$$

for $y < 0$. Where $b^2 = k_0^2 - a^2$, with $b \geq 0$ or $b/i \geq 0$ and $k_0 = 2p/l$, the modulus of the wave vector in vacuum. The first term is identified with the Fourier transform of the incident beam $E_i$ (incoming wave) with $A(a)$ its magnitude. The term with $B(a)$ represents the scattered wave; the transmitted wave is the term with the coefficient $C(a)$. Observe that, because an incident wave from $y < 0$ does not exist and since the field should be bounded for $y \to \pm\infty$, we should impose $D(a) = 0$ for every $a$. Now, from Eqs. (2) to (5) and the above discussion, it follows that the electric fields $E_1$ and $E_2$ are given by the following angular plane-wave expansion

$$E_1(x,y) = \frac{1}{\sqrt{2p}}\int_{-k_0}^{k_0} A(a)e^{i(ax-by)}da + \frac{1}{\sqrt{2p}}\int_{-\infty}^{\infty} B(a)e^{i(ax+by)}da \qquad (6)$$

(*for y>0*), and

$$E_2(x,y) = \frac{1}{\sqrt{2p}}\int_{-\infty}^{\infty} C(a)e^{i(ax-by)}da \qquad (7)$$

(*for y<0*)

Let $E_3(x,y)$ be the electric field in the slits ($y = 0$). The infinite conductivity of the screen requires the electric field be null on the slit separations, so $E_3$ can be expressed as

$$E_0(x,0) = \sum_{n=1}^{\infty} a_{n1} f_{n1}(x) + ... + \sum_{n=1}^{\infty} a_{nN} f_{nN}(x) \qquad (8)$$

where the functions $f_{np}(x)$ $(p = 1,2,3,..., N)$ are given by

$$f_{np} = \begin{cases} sin[x-(p-1)D]\dfrac{np}{\ell} & \text{if } (p-1)D \leq x \leq \ell + (p-1)D \\ 0 & \text{elsewhere} \end{cases} \qquad (9)$$

which satisfies

$$\langle f_{np}, f_{mq} \rangle = \int_{-\infty}^{\infty} f_{np} f_{mq}^{*} dx = \frac{\ell}{2} d_{nm} d_{pq} \ , \qquad (10)$$

with $n, m = 1,2,...\infty$, and $p, q = 1,2,..., N$. At this point, three different expressions for the total electric field given by Eqs. (6),(7) and (8), valid in three different regions, have been obtained; the final step is the determination of the functions $B(a), C(a)$, and the set of modal constants $a_{n1}, a_{n2}, ..., a_{nN}$. In order to determine these unknowns the requirement that the tangential component of the electric field be continuos at $y=0$ will be applied.

### 2.2 Conditions of continuity

From the continuity of the electric fields $E_1$ and $E_3$ at $y = 0$, we obtain from Eqs. (4),(5) and (8):

$$A(a) + B(a) = \sum_{n=1}^{\infty} a_{n1} \hat{f}_{n1}(a) + .... + \sum_{n=1}^{\infty} a_{nN} \hat{f}_{nN}(a) \qquad (11)$$

$$C(a) = \sum_{n=1}^{\infty} a_{n1} \hat{f}_{n1}(a) + ... + \sum_{n=1}^{\infty} a_{nN} \hat{f}_{nN}(a), \qquad (12)$$

where $\hat{f}_{np}(a)$ is the Fourier transform of $f_{np}(x)$ given by

$$\hat{f}_{np}(a) = e^{-ia[(p-1)D]} \frac{n\sqrt{p}}{\sqrt{2}\ell} \left[ \frac{1-(-1)^n \exp(-ia\ell)}{\left(\frac{np}{\ell}\right)^2 - a^2} \right], \qquad (13)$$

with $p = 1,2,3,4,..., N$ and $n = 1,2,3,4,..., \infty$. The above expressions provide us with two linear equations with an infinite number of unknowns $B(a), C(a)$, and $a_{np}$. This problem has been numerically solved by truncating the system to a finite order $N_0$ chosen until stability of the results is obtained and the conservation of energy is satisfied within a precision of better than $10^{-4}$. This procedure results into a system with $N_0 \times N + 2$ unknowns, so $N_0 \times N$ more equations are necessary. The continuity of the normal derivative of $E$ at $y=0$ give us the required equations, hence

$$\left\langle \frac{\partial E_1}{\partial y}(x,0) - \frac{\partial E_2}{\partial y}(x,0), f_{mq}(x) \right\rangle = 0 \qquad (14)$$

.

Now, applying the Parseval-Plancherel theorem $\langle f(x), g(x)\rangle = \left\langle \hat{f}(a), \hat{g}(a) \right\rangle$ to Eq. (14) we get

$$\left\langle \frac{\partial \hat{E}_1}{\partial y}(a,0) - \frac{\partial \hat{E}_2}{\partial y}(a,0), \hat{f}_{mq}(a) \right\rangle = 0 \qquad (15)$$

with $q = 1,2,...,N$, and $m = 1,2,...,N_0$. Thus Eq. (15) give us the remaining equations. After differentiating Eqs. (4) y (5) and replacing them into Eq. (15) the coefficients $B(a)$ and $C(a)$ are eliminated using Eqs. (11) y (12), and the following finite system is obtained in the unknowns $a_{np}$.

$$\sum_{n=1}^{N_0} a_{n1} \left\langle b\, \hat{f}_{n1}, \hat{f}_{mq} \right\rangle + ... + \sum_{n=1}^{N_0} a_{nN} \left\langle b\, \hat{f}_{nN}, \hat{f}_{mq} \right\rangle = \left\langle bA(a), \hat{f}_{mq} \right\rangle \qquad (16)$$

with $n, m = 1,2,...,N_0$, and $q = 1,2,...,N$. Let $a^1, a^2, ..., a^N$ be column-matrices consisting of the modal coefficients $a_{np}$, thus

$$\begin{aligned} &M^{11}a^1 + M^{12}a^2 + ... + M^{1N}a^N = S^1 \\ &M^{21}a^1 + M^{22}a^2 + ... + M^{2N}a^N = S^2 \\ &... \\ &M^{N1}a^1 + M^{N2}a^2 + ... + M^{NN}a^N = S^N \end{aligned} \qquad (17)$$

with

$$\left[M^{pq}\right]_{nm} = M^{pq}_{nm} = \int_{-\infty}^{\infty} b\, \hat{f}_{np}\, \hat{f}^{*}_{mq}(a)\, da \,, \qquad (18)$$

and

$$\left[S^{q}\right]_{m} = S^{q}_{m} = 2i \int_{-k_0}^{k_0} bA(a)\, \hat{f}^{*}_{mq}(a)\, da \,, \qquad (19)$$

with $b(a) = \sqrt{k_0^2 - a^2}$ as above. The matrix $M^{pq}$ is given by Eq. (18) and contains the opto-geometrical parameters of the system, and $S^q$ is a column-matrix linearly depending on $A(a)$. Solving numerically Eq. (17) by a matrix inversion method we determine the modal coefficients $a_{np}$, and thus the electric field inside the slits by means of Eq. (8). Substituting these $a_{np}$ into Eqs. (11) and (12) we have the amplitudes $B(a)$ and $C(a)$. Finally, by inserting these amplitudes into Eqs. (6) and (7) we get the scattered and diffracted fields, respectively; hence the solution of the problem is formally obtained.

*2.3 Conservation of energy*

Let $t$ be the transmission coefficient defined as the ratio between the transmitted energy through the *N* slits and the incoming energy. Similarly, let $r$ be the reflection coefficient defined as the ratio between the scattered energy and the incident energy. The conservation of the energy is thus written as

$$r + t = 1 \,. \qquad (20)$$

These quantities can calculated using the Poynting vector [3] as

$$t = \frac{\int_{-k_0}^{k_0} b(a)\left|C(a)\right|^2 da}{\int_{-k_0}^{k_0} b(a)\left|A(a)\right|^2 da} = \frac{\mathrm{Re}\left\{\sum_{p=1}^{N}\sum_{n=1}^{\infty} a^{*}_{np} S^{p}_{n}\right\}}{\int_{-k_0}^{k_0} b(a)\left|A(a)\right|^2 da} \qquad (21)$$

and

$$r = \frac{\int_{-k_0}^{k_0} b(a)\left|B(a)\right|^2 da}{\int_{-k_0}^{k_0} b(a)\left|A(a)\right|^2 da} = \frac{\int_{-k_0}^{k_0} b(a)\left\{\left|C(a) - A(a)\right|^2\right\} da}{\int_{-k_0}^{k_0} b(a)\left|A(a)\right|^2 da} \,. \qquad (22)$$

Besides, the scattered intensity as a function of the angle $q$ (see Fig. 1) in the far-field approximation can be expressed as [3]

$$I(q) = \frac{k_0^2}{2m_0 w} \sin^2 q \left| \hat{E}_3(k_0 \cos q, 0) \right|^2 \,. \qquad (23)$$

Before continue with the next Section, we call attention to the fact that every intensity pattern will be normalized to the incident energy $I_0$, i.e. the ratio $I(q)/I_0$ will be plotted.

**3. Numerical results**

As an incident electromagnetic beam wave, the two-dimensional version of a Gaussian beam shape will be considered. On the screen, and at normal incidence, the intensity of this field is given by

$$I(x, y = 0) = \exp\left[ -\frac{4(x-b)^2}{L^2} \right] . \qquad (24)$$

The position of the incident finite beam with respect to the *Oy* axis (alignment) is determined by the parameter *b* (see Fig. 1). *L* denotes the local (*1/e*)-intensity Gaussian beam diameter (*L*-spot diameter) which is a basic beam parameter. Unless otherwise is indicated, throughout the paper the beam position will be maintained fixed at $b = \Lambda/2$, with $\Lambda = N\ell + (N-1)d = ND - d$ the length of the system formed by *N* slits, i.e. the beam will be focused at the center of the finite line-grating. Besides, we call attention to the fact that the present theory is valid not only for Gaussian beams, but also Hermite-Gaussian [6,8,20-24], Gauss-Laguerre [25], Bessel [26], Bessel-Gauss [26,27], and even fractal-shape beams.

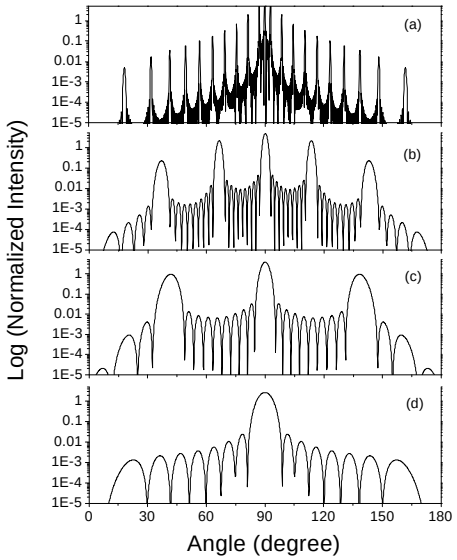


**Figure 2.** Logarithm of the diffracted intensity normalized to the total incident energy $\log(I(q)/I_0)$ for *10* slits of normalized period $D/\ell = 2.0$. With $L/\ell = 20/\sqrt{2}$, $b/\ell = 9.5$ and wavelengths (a) $l/\ell = 0.1$, (b) $l/\ell = 0.8$, (c) $l/\ell = 1.5$, and (d) $l/\ell = 2.5$.

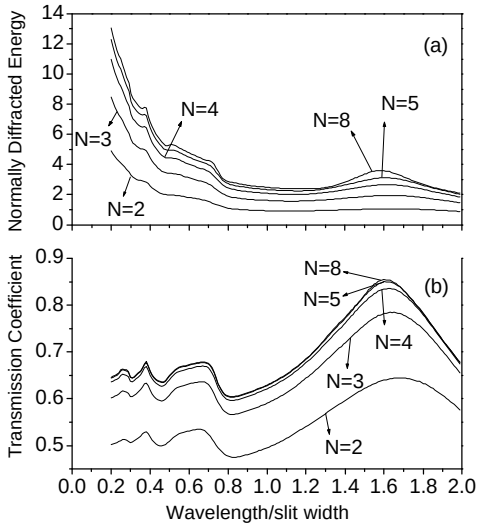


**Figure 3.** (a) Intensity diffracted at normal direction normalized to the total incident energy $(E/I_0)$, and (b) transmission coefficient $t$ dependence on the wavelength for 2,3,4,5, and 8 slits of period $D/\ell = 1.5$. With $L/\ell = 5/\sqrt{2}$ and beam positions $b/\ell = 1.25, 2.0, 2.75, 3.5$ and $5.75$, respectively.

In order to validate the method presented here, we have performed calculations for several systems previously reported in the literature. We have therefore compared the Otsuki´s results [20] for the diffraction of normally incident plane waves by several slits, with those obtained with a very wide spot ($L = 5000/\sqrt{2}$). The spectra are plotted in Figs. 2,3 and 4 of Ref. [20] for two, four and six slits of normalized width 2 and slit separation 2 for several values of the wave number $k_0$. The agreement is quite good. Moreover, our numerical results are also in good agreement with the experimental data reported by Lazar and DeAcetis [28] for two strips, as can be seen in Figs. 5 and 7 of Ref. [28].

### *3.1 Influence of the wavelength*

First, the influence of the wavelength on the diffraction will be investigated. Figures 2a, 2b, 2c and 2d show in a semilog-scale the spectra from ten slits of spacing (normalized to the slit width) $D/\ell = 1.5$, when they are illuminated by a Gaussian beam of width $L/\ell = 20/\sqrt{2}$ with wavelengths $l/\ell = 0.1,\ 0.8, 1.5$ ,and $2.5$ respectively.

Fig. 2a shows that within the scalar region ($l/\ell = 0.1$) the spectrum is very oscillating, concentrating the energy within a small angular sector around the finite-grating normal. As the ratio $l/\ell$ increases toward the vectorial region the number of oscillations diminishes; because of this, the number of primary maxima (spectral orders) strongly reduces as well. So, two orders, one order and none order (different from the zero-th order) in Figs. 2b,2c, and 2d can be detected, respectively. Moreover, these orders become broader as the wavelength increases. Observe that *N-2* secondary maxima appear between orders, just as occurs in the scalar region, except close to the angular extremes $(0°$ and $180°)$ where this number is reduced. In addition, in comparing with the Rayleigh-Sommerfeld Theory (RST) [22], we have found that this scalar theory cannot precisely determine all the features of the spectra, particularly the number of primary maxima when the wavelength lies within the vectorial region. For instance, a second-order maximum at $q = 37.0006°$ for $l/\ell = 0.80$ in Fig. 2b cannot be predicted by the RST.

On the other hand, the normally diffracted energy $e$ is an important optic parameter seldom studied in the literature. To overcome this deficiency in Fig. 3a we plot $e$ as a function of the wavelength for 2,3,4,5 and 8 slits, and a Gaussian beam of width $L/\ell = 5/\sqrt{2}$. Within the interval considered $(0.2 \le l/\ell \le 2.0)$ a decreasing function can be observed with maxima located at $l/\ell = 0.3725, 0.5112,$ and $\overline{1.5784}$ (bar indicates the value for a slit). An increase in the number of slits *N* produces a corresponding increase in intensity, maintaining the overall shape constant. However, we may note that the last maximum slightly displaces backwards as the number of slits increases. We have found that the magnitude of the shift depends both on *N* as on the beam width. In addition, Fig. 3b shows the plot of the transmission coefficient as a function of the wavelength using the same parameters as above. Now, it is possible to observe an increasing behavior as a function of *N*, with maxima located at $l/\ell = 0.2702, 0.3725, 0.6312$ and $\overline{1.7620}$, and minima at ë$/\ell = 0.3150, 0.4587$ ,and $0.8325$. Thus our numerical results partially prove the statement made in Ref. [4] in the sense that the position of maxima and minima

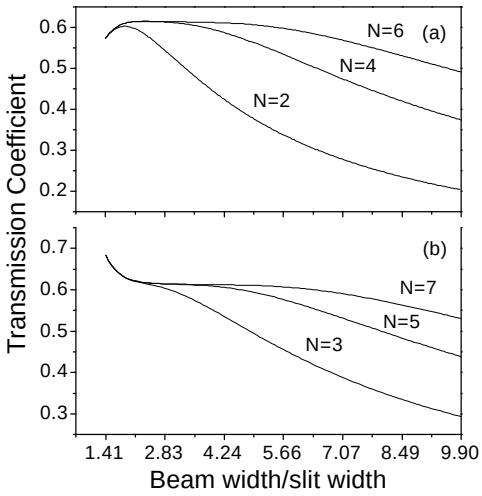


**Figure 4.** Transmission coefficient $t$ as a function of the normalized beam width $(L/\ell)$ for (a) 2,4,6 slits, and (b) 3,5,7 slits of period $D/\ell = 1.5$ with a wavelength $l/\ell = 0.9$. The beam waist is located at the middle of the finite grating, i.e. at (a) $b/\ell = 1.25, 2.75, 4.25$, and (b) $b/\ell = 2.0$, 3.5,5.0, respectively.

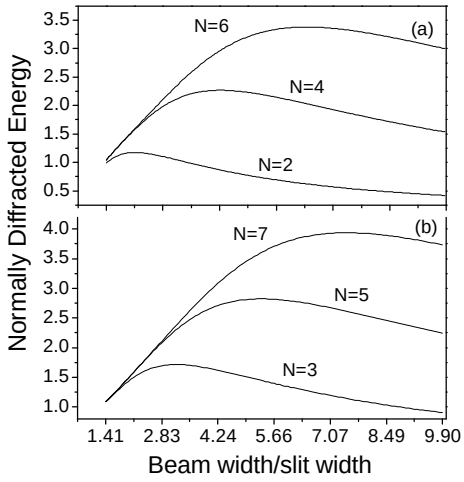


**Figure 5.** Intensity diffracted at normal direction normalized to the total incident energy $(E/I_0)$ as a function of the normalized beam width $(L/\ell)$. Parameters are set as in Fig. 5.

do not depend on the number of slits, since we have found that the last maximum actually depends not only on the number of slits but also on the beam width, i.e. on the illuminated area of the finite grating. The above conclusions indicate a very strong interference effect due to the vectorial character and due to the inhomogeneity of the incident wave. It is important to mention that this kind of oscillations cannot be predicted by any scalar theory.

*3.2 Influence of the beam width*

Now, the influence of the beam width $L/\ell$ on the transmission coefficient and on the normally diffracted energy is considered. Analysis will be divided into two parts, the first one for an even number of slits (Fig. 4a) and the second for an odd number (Fig. 4b). The first figure shows several maxima at $L/\ell = 1.8738, 2.3688,$ and $4.6668$ for 2,4 and 6 slits, respectively. Note that at the left of these values the curves converge at $(L/\ell)_{\min} = 1.7677$, and starting from this point the three curves decreases as one. This means that for widths lower than $(L/\ell)_{\min} = 1.7677$ the energy is transmitted in the same way no matter what the number of slits is. The rapid decreasing behavior in the transmission coefficient can be explained by the fact that when the number of slits is even, the beam is centered on a separation, so that when the beam gets narrower the reflectivity rapidly increases due to the infinite conductivity of the screen. Otherwise, for widths greater than $(L/\ell)_{\min}$, the transmission coefficient decreases, asymptotically converging to zero when the beam width becomes infinite (resembling a plane wave). This behavior can be easily understood if we note that once the system is covered by the field, the transmitted energy practically remains constant (for a fixed wavelength), whereas the incident energy increases. In the second case for N=3,5 and 7, Fig. 4b shows no maximum but rather a saddle point to which all curves converge. This point is also located very close to $(L/\ell)_{\min} = 1.7677$. In this case the curves show a growing behavior when the beam width $L/\ell < (L/\ell)_{\min}$. Now, the beam is centered over a slit so, when the beam gets narrower the transmitted energy increases. It is interesting to observe that the maximum and the saddle point correspond to values below the finite-grating length $\Lambda$.

This means that it is not necessary that the $L/\ell$-spot diameter totally covers the finite-grating to obtain a maximum efficiency in the transmitted energy.

The normally diffracted energy $e$ as a function of the beam width is depicted in Fig. 5. Maxima are found at positions $L/\ell = 2.1213, 4.2426$ and $6.3640$ for 2,4 and 6 slits, respectively (Fig. 5a), whereas for 3,5 and 7 slits are located at $L/\ell = 3.1820, 5.3033$ and $7.4247$ (Fig. 5b). Note that these maxima are obtained when the width of the Gaussian beam completely covers the system as an integer number of periods, i.e. when $L/\ell = ND/\sqrt{2}$.

Finally, and regarding diffraction, our simulations show that the spectral features depend basically on the beam width $L/\ell$, i.e. on the illuminated area of the finite-grating.

*3.3 Influence of the beam position*

The influence of the beam position $b$ on the transmission coefficient and on the normally diffracted energy $e$ is shown in Figs. 6a and 6b, respectively for $l/\ell = 0.90$ and $L/\ell = 7/\sqrt{2}$. From Fig. 6a we may observe that the maximum on the transmission is achieved when the beam waist is perfectly centered on the system, which correspond to the maximum transmitted power position (the beam is

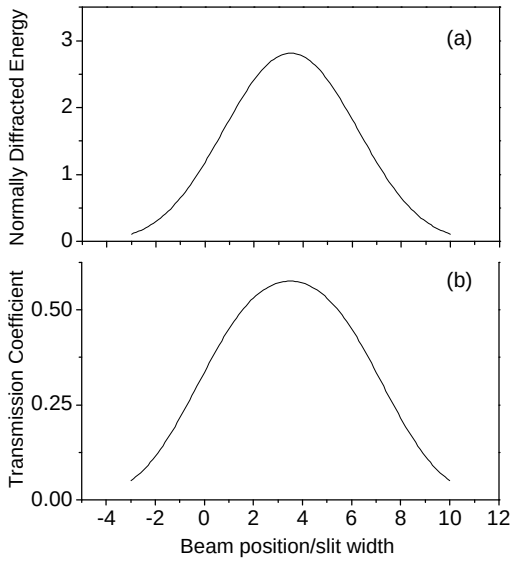


**Figure 6.** (a) Intensity diffracted at normal direction normalized to the total incident energy $\left(\mathrm{E} / I_0\right)$ and (b) transmission coefficient $t$ versus the normalized beam position $\left(b / \ell\right)$ for a finite grating with $N = 5$ and period $D / \ell = 1.5$. With $l / \ell = 0.9$ and $L / \ell = 7 / \sqrt{2}$.

over an aperture). When we move out from this point the magnitude of $t$ asymptotically decreases to zero.

Additional simulations for N>5 and different values of $l / \ell$ (not shown) lead us to conclude that the transmission coefficient adopts a Gaussian shape which maximum amplitude depends on the wavelength, on the beam width and on the number of slits as well, whereas its own width is directly proportional to the total incident energy. A similar behavior is followed by the normally diffracted energy as can be noted in Fig. 6b.

Regarding spectra, these do not show an important change in form, only a slight decrease in intensity can be noticed as the beam waist moves away from the finite-grating symmetry position.

## 4. Conclusions

A rigorous modal theory for solving the diffraction of Gaussian beams by N equally spaced slits ruled on an otherwise planar perfectly conducting surface was presented. The case of T.E.-polarization and normal incidence was considered. The study has been particularly carried out in the vectorial region, where the polarization effects are important. The far-field radiation pattern, the transmission coefficient and the energy diffracted normally to the screen were analyzed as a function of several optogeometrical parameters. The parameters considered were the wavelength, and the beam width as well as the beam position.

## Acknowledgments

The authors OMM and FChR thank support from COFAA-IPN.
This paper was partially supported by the CONACyT-Mexico and UAEM under grants I35695-E and 1527/2001, respectively.

## References

[1] Jeffrey J. Regan and David R. Andersen, Computers in Physics **49**, (Jan/Feb. 1991).
[2] O. Mata-Mendez, Opt. Lett **16,** 1629 (1991).
[3] O. Mata-Mendez, Rev. Mex. Fis. **38,** 850 (1992).
[4] O. Mata-Mendez and F. Chavez-Rivas, Rev. Mex. Fis. **39,**706 (1993).
[5] O. Mata-Mendez, Phys. Rev. B **37,** 8182 (1988).
[6] A. Zuñiga-Segundo and O. Mata-Mendez, (Rapid Comm.) Phys. Rev. B **46,** 536 (1992) .
[7] A. Sasaki , Jpn. J. Appl. Phys. **19**,1195 (1980).
[8] O. Mata-Mendez, M. Cadilhac, and R. Petit, J. Opt. Soc. Am.**73**, 328 (1983).
[9] Kojima T. .J. Opt. Soc. Am. A **7**,1740 (1990).
[10] P. Langlois, A. Boivin, and R. A. Lessard, J. Opt. Soc. Am. A **2**, 858 (1985).
[11] Kraus H.G. , J. Opt. Soc. Am. A **7**,47 (1990).
[12] D. Marcuse, Light Transmission Optics, (Van Nostrand Reinhold Co., New York, 1982).
[13] J. B. Keller, J.Opt. Soc. Am. **52,** 1629 (1962) .
[14] E. Loewen and E. Popov, Diffraction gratings and applications, (Marcel Dekker, Inc.,New York, 1997).
[15] D. L. Jain and R. P. Kanwal, Can J. Phys. **50**, 928 (1972).
[16] R. P. Kanwal and B. K. Sachdeva, Z. Angew. Math. Phys. **24**, 111 (1973).
[17] K. Saermak, Appl. Sci. Res. B **7**, 417 (1960).
[18] K. Saermak, Appl. Sci. res. B **8**, 29 (1960).
[19] K. Sachdeva and R. A. Hurd, Can. J. Phys. **53**, 1013 (1975).
[20] T. Otsuki, J. Opt. Soc. Am. **7**, 646 (1990).
[21] Em. E. Kriezis, P. K. Pandelakis, and A. G. Papagiannakis, J. Opt. Soc. Am. **11**, 630 (1994).
[22] O. Mata-Mendez and F. Chavez-Rivas, J. Opt. Soc. Am. A **15**, 2698 (1998).
[23] O. Mata-Mendez and F. Chavez-Rivas, J. Opt. Soc. Am. A **18**, 537 (2001).
[24] J. Serna, P. M. As and R. Nez-Herrero, Appl. Opt. **32**, 1084 (1993).
[25] S. Solimeno and A. Cutolo, Opt. Lett. **11**, 141 (1986).
[26] R. M. Herman and T. A. Wiggins, J. Opt. Soc. Am. A **17**, 1021 (2000).
[27] S. Ruschin and A. Leizer, J. Opt. Soc. Am. A **15**, 1139 (1998).
[28] L. A. DeAcetis and I. Lazar, Appl. Opt. **12**, 2804 (1973).